Scripta Materialia 146 (2018) 60–63

Contents lists available at ScienceDirect

Scripta Materialia

journal homepage: www.elsevier.com/locate/scriptamat

Regular article

Advanced high strength steel (AHSS) development through chemical patterning of austenite

W.W. Sun, Y.X. Wu, S.C. Yang, C.R. Hutchinson *

Department of Materials Science and Engineering, Monash University, Clayton 3800, VIC, Australia

ARTICLE INFO

Article history:
Received 9 October 2017
Received in revised form 2 November 2017
Accepted 7 November 2017
Available online xxxx

Keywords:
Advanced high strength steels (AHSS)
Pearlite
Retained austenite
TRIP

ABSTRACT

A new approach for the development of medium Mn AHSS is proposed in this work. It exploits a fine scale (~100 nm) chemical patterning of Mn in austenite that may be obtained by the austenitisation of a pearlite structure formed under conditions with strong Mn partitioning between ferrite and cementite. The resulting 'ghost pearlite' ferrite/austenite can be subsequently treated to exhibit an interesting combination of ultimate tensile strength (UTS) (1600–2100 MPa) and ductility (7–10% elongation). The simple steel composition and very short processing provides a UTS-ductility combination similar to maraging steels and super bainitic steels.

Third generation advanced high strength steels (AHSS) are multiphase composite materials that exploit the stress or strain induced transformation of austenite to achieve impressive combinations of ductility and UTS. The materials contain much less Mn than the fully austenitic, second generation AHSS, but more than the first generation AHSS (e.g. TRIP steels) and are therefore often referred to as 'medium Mn' steels. A critical aspect of their design is the control of austenite stability so that its transformation into martensite is tuned as a function of temperature, strain and strain-rate to maximise the UTS-ductility combination obtained. The austenite stability depends on its size and shape, as well as the mechanical constraints imposed by the surrounding phases, but the dominant factor is its composition, particularly the C and Mn contents. The Quench and Partitioning treatment (Q + P) uses a low temperature (250–500 °C) [1] anneal to enrich the austenite in carbon by diffusion from the martensite in a martensite/austenite aggregate. This is almost always accompanied by some precipitation of carbides in the martensite so the partitioning of carbon to the austenite is incomplete and this must be accounted for in the alloy and process design. At such low temperatures, there is no long-range partitioning of the substitutional Mn in Q + P. Intercritical annealing is another approach where the alloy is first treated in the austenite + ferrite two phase field at elevated temperatures (600–900 °C) during which the austenite is enriched in both Mn and C, and the austenite then partially decomposes during cooling leaving some remaining metastable austenite. The final properties of the steels are very sensitive to the intercritical anneal and the starting structure of the alloy.

In this contribution, we present an alternative processing route for controlling both the stability and spatial distribution of metastable austenite in a ferritic matrix in medium Mn steels. The approach exploits the pearlite transformation at relatively low temperatures (<600 °C) to create a layered structure of ferrite and cementite. The cementite formed in steels with significant Mn contents is strongly enriched in Mn during the pearlite transformation [2], even when formed at low temperatures, because the Mn partitioning takes place in the transformation interface itself which acts as a short-circuit diffusion path. Mn enrichments in the cementite may reach the order of 40% [2]. The pearlite transformation is a fast transformation and strongly partitioned pearlite may form in the space of an hour or two at temperatures of 500–600 °C. If this partitioned pearlite is subsequently austenitised by a short thermal treatment at a suitable temperature, it is possible to obtain a fully austenitic state, but where the austenite retains the chemical patterning in Mn present in the pearlite. This has sometimes been referred to as 'ghost pearlite' [3,4]. When the chemically patterned austenite is cooled, it is possible to obtain a layered structure of ferrite/martensite and metastable austenite (enriched in Mn and C) with a length scale similar to the lamellar spacing of the pearlite. This creates a new type of multiphase microstructure of ferrite and metastable austenite that is both strong (due to the fine length scale) but also able to exploit the metastability of the austenite to obtain good ductility.[1] As will be shown, the structures and properties obtained bear resemblance to 'super bainite' structures although the processing requires 1–4 h of thermal treatments rather than days or months [5–8].

* Corresponding author.
E-mail address: christopher.hutchinson@monash.edu (C.R. Hutchinson).

[1] Towards the completion of this work, a similar design concept using pearlite as a starting structure was suggested by the group of Dr. Hao Chen (Tsinghua University) during the ALEMI meeting at Tsinghua University (2017).

https://doi.org/10.1016/j.scriptamat.2017.11.007
1359-6462/

To demonstrate the approach, we have used a medium carbon Fe-0.51C-4.35Mn (wt%) steel. At each stage of the process, both the tensile response and the microstructure have been characterised to illustrate the design rationale. To produce this steel, a hot-rolled and then cold-rolled Fe-0.1C-4.6Mn (wt%) alloy was carburized in an atmosphere of CO/CO_2 at 910 °C for 24 h. This carbon content was chosen so a 100% pearlitic microstructure could be formed on cooling. A fully pearlitic structure has been used to simplify the introduction of the concepts and the interpretation of the strain hardening behaviour. In this respect, the properties obtained should not be directly compared with 3rd Gen AHSS that have much lower carbon contents, although the concept introduced here can be easily extended to these steels and will be subsequently discussed.

Tensile tests were performed on an Instron 4505, operating with a crosshead speed of 0.02 mm/s and using a 10 mm extensometer. Tensile samples with a gauge length of 12 mm, width of 5 mm and thickness of 1 mm were prepared from the cold-rolled sheet using electric discharge machining. The microstructure, and particularly the partitioning of Mn, was characterised using scanning transmission electron microscopy (STEM, FEI Tecnai F20) equipped with energy-dispersive spectroscopy (EDS). TEM foils were prepared using a focussed ion beam (FIB). Phase fractions were determined using X-ray diffraction (XRD) and the data were collected with Co Kα radiation on a Bruker D8 advance diffractometer with a Lynxeye position sensitive detector. Samples were finished with colloidal silica suspension polishing. The XRD data was analysed using whole-pattern Rietveld method [9] as embodied in the software package TOPAS (version 5, Bruker AXS).

The initial pearlite was formed by furnace cooling from the carburization temperature of 910 °C directly to 575 °C and holding for 4 h. The samples had a relatively large prior austenite grain size of ~50 μm due to the carburization time and hence the need to hold for 4 h to obtain full pearlite transformation. In a material of more conventional prior austenite grain size of 10 μm, the pearlite transformation would be completed within ~1 h.

The engineering stress-strain curve from the fully pearlitic sample is shown in Fig. 1a. As will be shown in Fig. 2, this pearlite contains an interlamellar spacing of ~100 nm and Fig. 1 is a typical tensile response for pearlitic samples with similar lamellar spacings [10]. A bright field TEM image of the pearlite is shown in Fig. 2a. The interlamellar spacing is ~80 nm which is within the range of spacings observed by Marder and Bramfitt for eutectoid steels transformed at the same temperature [11]. An EDS line profile across the lamellae is shown in Fig. 2b demonstrating the strong partitioning of Mn to the cementite. U-fractions of Mn between 26 and 30% are obtained. This corresponds to 20–23 at.% Mn in the cementite and is close to the value expected from local equilibrium (27 at.%) in this composition at this temperature (calculated using Thermocalc and the TCFe8 database).

Tensile samples consisting of this fully pearlitic microstructure were reaustenitised at 770 °C (slightly above the Ac_3 of 760 °C measured using dilatometry) in a salt bath for 20 s followed by air cool. The tensile response of these samples can be seen in Fig. 1a. After re-austenitisation, the samples fail abruptly at a stress of around 1 GPa with limited plasticity. This is almost certainly due to the high carbon, brittle martensite formed during cooling from the re-austenitised state. A TEM micrograph showing the ferrite/martensite and thin austenite layered structure can be seen in Fig. 2c. The layer spacing in this image is 55 nm. The corresponding EDS line scan is shown in Fig. 2d. Some Mn redistribution has occurred in the austenite during the 20 s re-austenitisation, reducing the Mn enrichment to a U-fraction of 10%, but the chemical patterning developed by the initial pearlite transformation remains. The phase fractions present in this chemically patterned, layered microstructure have been quantified using XRD. The XRD pattern and the fit profile from full pattern Rietveld refinement are shown in Fig. 3a. The layered structure consists of ferrite and austenite, with an austenite fraction of 17.4% ± 1%. To obtain good fits in the refinement, it was necessary to include both BCC and BCT phases. This is not surprising and represents the ferrite formed diffusionally during the cool from the austenitisation temperature and the martensite.

To solve the issue of the brittleness of the chemically patterned and layered structures (Fig. 2c), the structures have been given a low temperature tempering. The re-austenitised and air cooled samples were tempered in a salt bath at temperatures between 300 °C and 500 °C for 30 s or 2 min followed by air cool. The tempering relaxes and slightly softens the martensite.

The tensile response of three tempering treatments are shown in Fig. 1a – 500 °C 2 min, 400 °C 30 s and 300 °C 30 s. These tempering treatments result in yield strength-UTS-ductility combinations of 1130 MPa–1550 MPa – 7%, 1190 MPa–1750 MPa – 10%, and 1030 MPa–2100 MPa – 7%, respectively.

Fig. 1b includes the Kocks-Mecking plots of the samples after the different treatment conditions, presenting the change in strain hardening rate ($d\sigma/d\varepsilon$) as a function of true stress. The sample tempered at 500 °C for 2 min (green curve) shows a slight TRIP effect at 800–1200 MPa true stress (Fig. 1b). Although the TRIP effect is not as obvious as in the reaustenitised samples without tempering, the decrease in the strain hardening rate is significantly slower than that of the initial pearlite. This relatively high tempering temperature of 500 °C leads to austenite decomposition and the volume fraction of austenite prior to the tensile test is measured by XRD to be only 3.5–4% (Table 1) and all of it transformed during the tensile test.

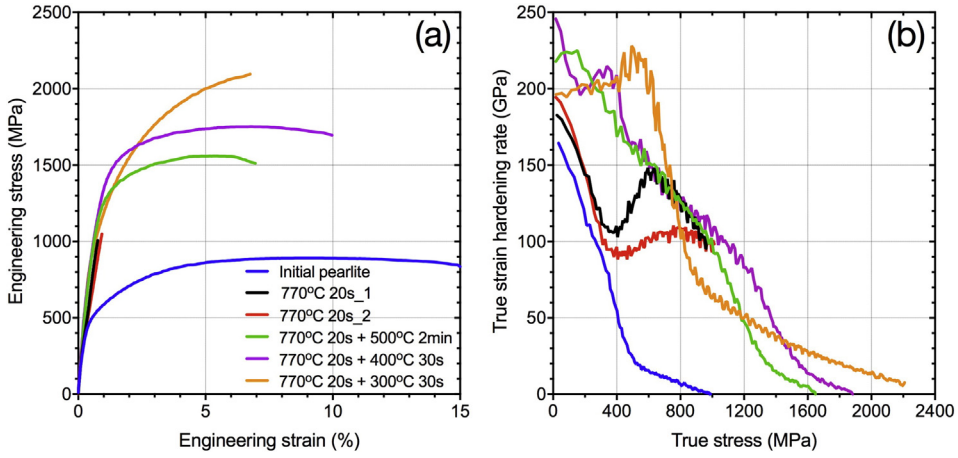

Fig. 1. (a) Engineering stress-strain curves, and (b) Corresponding true strain hardening rate versus true stress curves (Kocks-Mecking plots). (For interpretation of the references to color in this figure, the reader is referred to the web version of this article.)

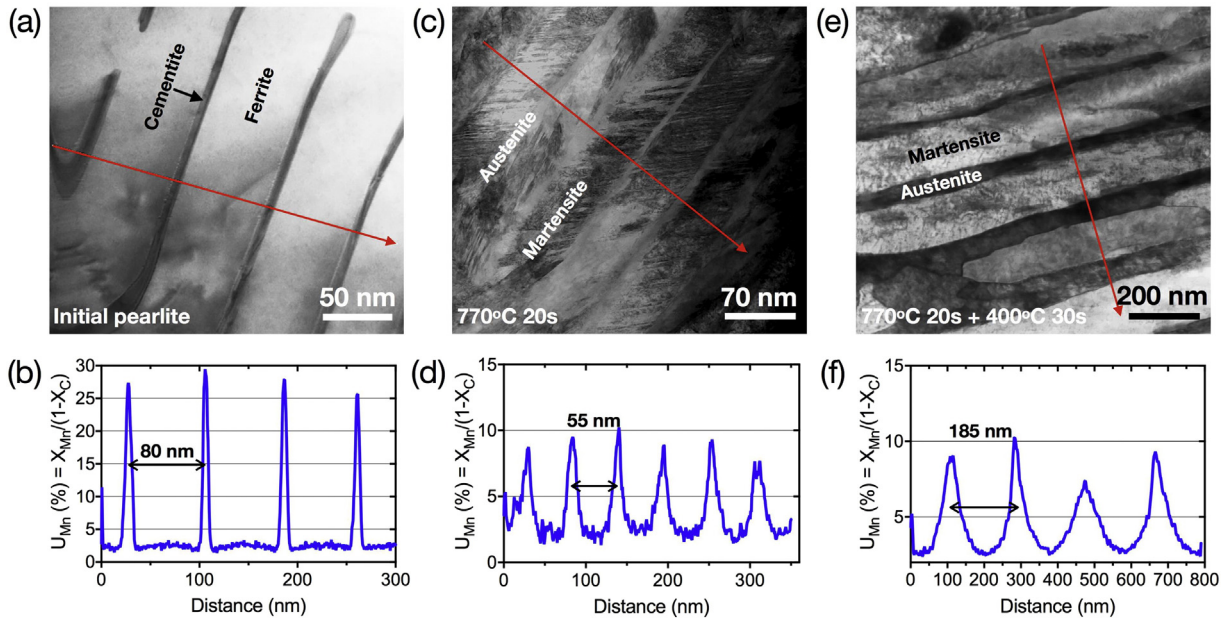

Fig. 2. STEM bright field images and EDS line scans of a, b) initial pearlite, c, d) pearlite reaustenitised at 770 °C for 20 s followed by air cool and e, f) pearlite tempered at 400 °C for 30 s after re-austenitisation.

The tempering treatment of 400 °C for 30 s provides a very interesting yield strength-UTS-ductility combination of 1190 MPa–1750 MPa-10%. This condition shows a more pronounced TRIP effect at higher stress levels (~1200 MPa) (purple curve, Fig. 1) compared to the samples tempered at 500 °C. A bright field TEM micrograph of the sample after 400 °C tempering is shown in Fig. 2e. The restored deformation structure in the ferrite/martensite region due to the tempering can be seen by comparing Fig. 2c and e. The EDS line profile in Fig. 2f demonstrates the Mn chemical patterning after the re-austenitisation and tempering at 400 °C for 30 s. In this case, the chemical patterning has a spacing of 185 nm, compared with 55 nm in Fig. 2c and 80 nm in Fig. 2a. These pattern spacings are a reflection of the distribution of lamellar spacings present in the initial pearlite, even when formed under isothermal conditions. Such spreads in lamellar spacings are consistent with previous reports [12,13]. The chemical patterning of Mn highlights an important advantage of this processing approach – by controlling the re-austenitisation and tempering treatments, the Mn diffusion profile may be specifically tailored to provide a controlled spectrum of austenite stabilities, for example for controlled transformation as a function of straining.

The corresponding XRD pattern in Fig. 3b shows sharpened BCC reflections (cf. Fig. 3a). As anticipated, this shows that the tempering of martensite regions is beneficial to avoid the premature failure. Compared to the 500 °C tempered sample, the major difference is that 400 °C tempered sample is able to generate additional strain hardening at stresses higher than 800 MPa.

The volume fraction of retained austenite in the 400 °C tempered sample is 9–10% (Fig. 3b and Table 1), and all of it has been utilized for the TRIP effect during the tensile test since no retained austenite is detectable in XRD of the fractured gauge (Fig. 3c).

If instead the tempering is performed at 300 °C for 30 s, the yield strength is ~1 GPa, the UTS is 2.1 GPa and the total elongation is ~7% (Fig. 1a). These properties are comparable to the mechanical properties of nanobainite (e.g. yield strength 1–1.5 GPa and UTS 1.5–2 GPa [14]), which requires heat treatments in the range of 125 °C and 325 °C for many days [6,15].

The strain hardening behaviour (orange curve, Fig. 1b) of the 300 °C tempered sample is different to those tempered at 400 °C and 500 °C. The strain hardening rate is higher at lower stress level but continuously decreases without a discernible hump when stress increases. The

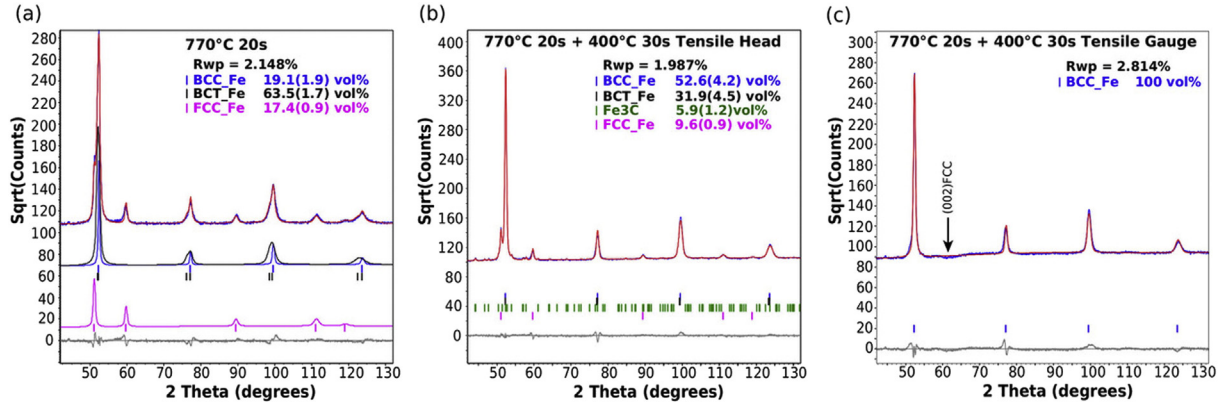

Fig. 3. Selected XRD patterns measuring austenite (FCC) fractions at different stages of heat treatments and tensile tests: (a) after intercritical annealing at 770 °C for 20 s followed by air cool, sample containing ~18.5% austenite. After intercritical annealing at 770 °C for 20 s followed by air cool and tempered at 400 °C for 30 s, (b) austenite reduced to 9.69 vol% during tempering and (c) all the austenite transformed after deformation. Phase fractions are reported for each condition and the Rietveld errors are included in the bracket.

Table 1
Austenite volume fractions measured using XRD after different heat treatments and tensile tests.

Sample description	Austenite volume fraction (%)
770 °C 20 s: Tensile head	17.4 ± 1
770 °C 20 s + 500 °C 2 min: Tensile head	3.8 ± 1
770 °C 20 s + 500 °C 2 min: Tensile gauge	None
770 °C 20 s + 400 °C 30 s: Tensile head	9.6 ± 1
770 °C 20 s + 400 °C 30 s: Tensile gauge	None
770 °C 20 s + 300 °C 30 s: Tensile head	22.6 ± 2
770 °C 20 s + 300 °C 30 s: Tensile gauge	11.1 ± 1

differences come from the amount and local chemistry of retained austenite and how it transforms with strain. The volume fraction of the retained austenite after tempering at 300 °C is ~22% (Table 1), which is similar to the as-austenitised sample. 300 °C is a temperature where the brittle martensite can be relaxed but the stability of retained austenite can be maintained. When the fractured gauge is examined by XRD, only half of the austenite is TRIPed during tensile deformation in the 300 °C tempered sample (Table 1) and the stress-strain curve did not reach Considere's criterion before failure. A better combination of strength and elongation will be possible by dedicated studies to control the stability (and stability distributions) of the austenite.

Interesting combinations of strength and ductility were obtained in this study using the chemical patterning of austenite from an initial pearlite microstructure with Mn enriched cementite lamella. De Moor et al. [15] have summarised strategies for developing third generation AHSS and the mechanical properties (elongation versus UTS) resulting from different processing approaches. The approach of chemical patterning of austenite to produce AHSS is capable of producing UTS-ductility combinations in the property range shown by ultrafine bainitic steels. Morphologically, the fine chemically patterned austenite provides high strength but also geometric constraints to improve the austenite stability. The simple composition used in this study also coincides with the cost-efficient perspective that is one of driving forces of developing the third generation AHSS and the gradient profiles in Mn (Fig. 2) provides an opportunity for tailing not only the average austenite stability but also the distributions of stability. This approach may potentially be coupled to industrial steel sheet production lines, in which partitioned pearlite can be formed from the hot rolling step during coiling. The re-austenitization and short time annealing (within 1 min) is fully compatible with existing continuous annealing.

A fully pearlitic structure has been used in this study to simplify the introduction of the concepts and the interpretation of the strain hardening behaviour. However, for low carbon grades of medium Mn steels, instead of generating a fully pearlitic microstructure, one could explore an initial microstructure of hypoeutectoid ferrite and fine pearlite. After re-austentitisation one may then obtain islands of chemically patterned Mn in a sea of more uniform Mn – leading to different combinations of ferrite/austenite aggregates. In this second level of composite, the softer hypoeutectoid ferrite would further act to accommodate the deformation of the brittle martensite that may form from the chemically patterned austenite during cooling from elevated temperatures and tempering may not be required at all.

There are many aspects of this new approach that need to be studied. The amount of retained metastable austenite is primarily determined by the reaustenitisation of the initial pearlite and the partitioning present in the initial pearlite can be manipulated by controlling the bulk alloy composition and transformation temperature. The austenitisation temperature and time should be suitable to balance a sufficient fraction of retained austenite and austenite stability controlled by Mn and C content. In the as-austenitised ghost pearlite sample, cementite is not 100% dissolved during the short austenitisation (even though the volume fraction is so low it cannot be measured by XRD) and presents as a small fraction of small globules embedded in the austenite lamellae. Based on the present results, it is worth increasing the reaustenisation time or using slightly higher temperatures to fully dissolve the cementite and free the Mn to a larger extent to austenite. From the 300 °C tempering shown, tempering is capable of relaxing the martensite and retaining the austenite fraction (similar to the Q&P process). It is to be further explored to investigate the embrittlement susceptibility and refine the TRIP mechanism in the final state of microstructure.

In summary, a new processing route for medium Mn AHSS has been proposed, which aims to control both the stability and spatial distribution of metastable austenite in a ferrite matrix. An ultra-fine layered structure of austenite and ferrite is created through a short re-austenitisation and tempering of pearlite, in which Mn retains in the thin austenite lamellae forming layered patterns. This new type of multiphase microstructure containing ferrite and metastable austenite is both strong (1600–2100 MPa) and shows good ductility (7–10% elongation), opening a door to novel microstructural design concepts of the third generation AHSS.

The authors gratefully acknowledge the support of the Australian Research Council (ARC) and ArcelorMittal and in the form of an ARC Linkage Grant (LP150100756). In particular, CRH would like to thank Dr. Artem Arlazarov, Prof. Chad Sinclair and Mr. Lingyu Wang for fruitful discussions and suggestions. YXW gratefully acknowledges the award of the Australian Government Research Training Program Scholarship. The authors would also like to express thanks for the use of equipment within the Monash Centre for Electron Microscopy, Monash X-Ray Platform as well as Deakin University (Dilatometer was trained by Mr. Jerome Cornu).

References

[1] D.V. Edmonds, K. He, F.C. Rizzo, B.C. De Cooman, D.K. Matlock, J.G. Speer, Mater. Sci. Eng. A 438 (2006) 25.
[2] C.R. Hutchinson, R.E. Hackenberg, G.J. Shiflet, Acta Mater. 52 (2004) 3565.
[3] G.R. Speich, A. Szirmae, M.J. Richards, Trans. Metall. Soc. AIME 245 (1969) 1063.
[4] J.L. Cunningham, D.J. Medlin, G. Krauss, J. Mater. Eng. Perform. 8 (1999) 401.
[5] H.K.D.H. Bhadeshia, Nanostructured Bainite, Proceedings of the Royal Society of London A: Mathematical, Physical and Engineering Sciences, vol. 466, The Royal Society, 2010 3.
[6] F.G. Caballero, H.K.D.H. Bhadeshia, Curr. Opinion Solid State Mater. Sci. 8 (2004) 251.
[7] F.G. Caballero, H.K.D.H. Bhadeshia, K.J.A. Mawella, D.G. Jones, P. Brown, Mater. Sci. Technol. 18 (2002) 279.
[8] C. Garcia-Mateo, F.G. Caballero, H.K.D.H. Bhadeshia, ISIJ Int. 43 (2003) 1821.
[9] H.M. Rietveld, J. Appl. Crystallogr. 2 (1969) 65.
[10] M. Dollar, I.M. Bernstein, A.W. Thompson, Acta Metall. 36 (1988) 311.
[11] A.R. Marder, B.L. Bramfitt, Metall. Trans. A. 7 (1976) 365.
[12] G.F. Vander Voort, A. Roósz, Metallography 17 (1984) 1.
[13] J.F. Tilbury, T.D. Mottishaw, G.D.W. Smith, Metallography 19 (1986) 243.
[14] C. Garcia-Mateo, F.G. Caballero, ISIJ 45 (2005) 1736.
[15] E. De Moor, P.J. Gibbs, J.G. Speer, D.K. Matlock, J.G. Schroth, Iron Steel Technol. 7 (2010) 132.